Mechanical Properties and Microstructure of Neutron Irradiated Cold-worked Al-1050 and Al-6063 Alloys

A. Munitz, C. Cotler and M. Talianker

1. Abstract

The impact of neutron irradiation on the internal microstructure, mechanical properties and fracture morphology of cold-worked Al-1050 and Al-6063 alloys was studied, using scanning and transmission electron microscopy, and tensile measurements. Specimens consisting of 50 mm long and 6 mm wide gauge sections, were punched out from Al-1050 and Al-6063 23% cold-worked tubes. They were exposed to prolonged neutron irradiation of up to $4.5x10^{25}$ and $8x10^{25}$ thermal neutrons/m^2 ($E < 0.625$ eV) for Al-6063 and Al-1050, respectively, at temperatures between 41 and 52°. The tensile specimens were then tensioned until fracture in a hydraulic tension machine at a strain rate of $2x10^{-3}$ s^{-1}. In general, the uniform and total elongation, the yield stress, and the ultimate tensile strength increase as functions of fluence. However, for Al-1050 a decrease in the ultimate tensile strength and yield stress was observed up to a fluence of $1x10^{25}$ thermal neutrons/m^2 which then increase with thermal neutrons fluence. Metallographic examination and fractography for Al-6063 revealed a decrease in the local area reduction of the final fracture necking. This reduction is accompanied by a morphology transition from ductile transgranular shear rupture to a combination of transgranular shear with intergranular dimpled rupture. The intergranular rupture area increases with fluence. In contrast, for Al-1050, fracture morphology remains ductile transgranular shear rupture and the final local area reduction remains almost constant No voids could be observed in either alloy up to the maximum fluence. The dislocation density of cold-worked Al was found to decrease with the thermal neutron fluence.

Prolonged annealing of unirradiated cold-worked Al-6063 at 52° led to similar results. Thus, it appears that, under our irradiation conditions, whereby the temperature encompassing the samples increases the exposure to this thermal field is the major factor influencing the mechanical properties and microstructure of aluminum alloys.

2. Introduction

Aluminum alloys exhibit good corrosion resistance as well as very low capture cross-section of fast and thermal neutrons, and hence are used extensively as structural materials in the nuclear industry. In the past, the choice of a particular alloy was based on the properties of the unirradiated material[1]. Structural materials in the reactor core are exposed to large fluxes of fast and thermal neutrons, resulting in microstructural changes. Thus, changes in mechanical properties take place during service. Numerous studies have been conducted concerning the irradiation impact on aluminum alloy properties[1-19]. Irradiation usually induces degradation in mechanical properties (particularly increase of ultimate tensile strength and reduction of elongation), and swelling. On the other hand, irradiation of cold-worked Al-1050 results in its annealing, and consequently the ultimate tensile strength and elongation increase with the neutron fluence[17]. Some studies indicate that annealing of cold-worked Al-1100[15] and Al-6061[1] may occur during irradiation. However, the impact of irradiation of cold-worked aluminum alloys on the mechanical properties is not well established, especially for alloys containing Mg, which undergo precipitation hardening. The present work was aimed at investigating the post-irradiation properties of cold-worked Al-6063 and Al-1050.

3. Experimental

Al-6063 and Al-1050 23% cold-worked parts were exposed to prolonged irradiation of neutron fluences of up to 4.5×10^{25} and 8×10^{25} thermal neutrons/m^2 ($E < 0.625$ eV), respectively at a temperature range of 41 to 52°. For mechanical examination, tensile specimens consisting of 50 mm long and 6 mm wide gauge sections were punched out from the parts. In the case of Al-1050, specimens annealed for 5h at 500° were also checked. According to our past experience regarding transmission electron microscopy (TEM) of punched samples, punching never introduces any significant work hardening. Following this step, the samples were strained in a hydraulic tension machine at a rate of 2×10^{-3} s^{-1} until fracture was detected. Fractured surfaces were examined with a scanning electron microscope (SEM). Parts of the aluminum were thinned for TEM. First thinning to about 150 μm was performed chemically with a 1M aqueous solution of NaOH. Then, discs of 3 mm diameter were punched out of the specimen and further thinned by electropolishing at 20-30 V using 20% perchloric acid in methanol at -20°.

Structural materials in a reactor core are influenced not only by the fast and thermal neutron interaction, but undergo a prolonged low temperature annealing. In order to examine the effect of low-temperature annealing, a set of Al-6063 23% cold-worked samples were annealed at 52° for over 2.5 years. These samples were examined in the same way as the irradiated ones.

4. Results

4.1 Mechanical properties of irradiated aluminum

Irradiation of cold-worked Al-1050 and Al-6063 caused changes in their mechanical properties, the nature and extent of which depended on the thermal neutron fluence, as seen in Tables 1 - 3. Typical stress/strain curves of unirradiated, as well as irradiated Al-1050 and Al-6063 for different neutron fluences are presented in Figures 1 and 2, respectively. Differences exist between the two types of aluminum. For Al-1050 the ultimate tensile strength (σ_{UTS}) changed with irradiation (Table 1 and Figure 1); first it dropped below the unirradiated value to a minimum value of 95 MPa for fluences of less than 10^{25} thermal neutrons/m^2; then it rose with continued irradiation. At $5x10^{25}$ thermal neutrons/m^2, σ_{UTS} increases above the unirradiated value (123 MPa) to 133 MPa. The tensile strength increased further until it reached its ultimate value of 142 MPa at the maximum fluence exercised, $8x10^{25}$ thermal neutrons/m^2. The uniform elongation as well as the total elongation increased with increasing fluences for all zones (i.e., the uniform elongation increased from 2.7% for unirradiated samples to 15.1% for the maximum fluence). Many of the samples fractured outside the extensiometer. Therefore, the uncertainty in the total elongation is quite large. To gain a better understanding of the impact of irradiation on the mechanical properties, we also checked the mechanical properties of Al-1050 annealed for 4 h at 400 and 500° after irradiation (see Table 1).

The impact of irradiation on the mechanical properties of Al-6063 is somewhat different. As seen from Figure 2 and Table 2, the uniform elongation, the yield strength-σ_Y and the ultimate tensile strength-σ_{UTS} of cold-worked

Al-6063 increased with neutron fluence, whereas the final area reduction of the fracture decreased with this fluence. Generally, the total elongation was almost unchanged, with only a slight tendency for increase with the neutron fluence.

Table 1: Mechanical properties of cold-worked Al-1050 as a function of the thermal neutron fluence, compared with the cold-worked tubes and tubes annealed at different temperatures for 4 h.

Conditions		Stress		Elongation	
		σ_Y [MPa]	σ_{UTS} [MPa]	Uniform [%]	total [%]
Unirradiated and annealed for 4 h	As received	117	140	2.7	4.0
	400°C	43	72	32.0	36.0
	500°C	43	71	40.1	43.5
Irradiated [10^{25} n/m^2]	<1	83	95	4.0	4.8
	3	102	106	10.1	12.0
	5	120	133	8.0	11.8
	8	120	142	15.1	16.0

Fig. 1: Stress-strain curves of unirradiated and unirradiated and annealed for 4 h at 500°C of Al-1050 samples and of samples irradiated to different thermal neutron fluences.

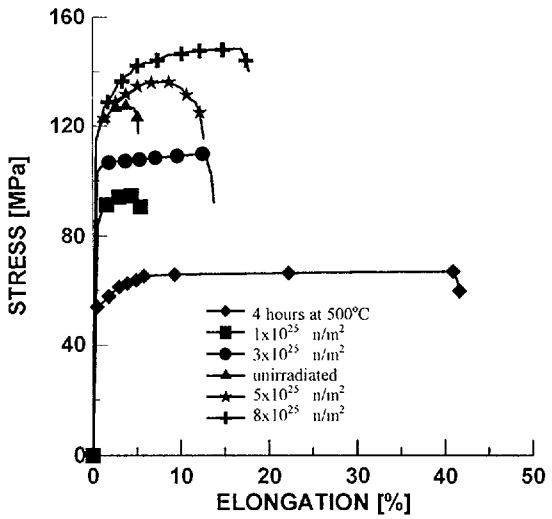

Fluence [10^{24} n•m^{-2}]	Stress		Elongation		Final area reduction
	σ_Y [MPa]	σ_{UTS} [MPa]	Uniform [%]	total [%]	[%]
0.0	189	239	7.9	11.5	73
1.5	222	291	9.6	11.0	50
4.7	222	282	11.2	13.5	45
8.8	234	289	10.6	13.4	47
11.5	224	277	9.7	11.2	45
14.9	240	301	12.3	13.5	43
19.0	235	294	11.3	14.1	35
21.5	236	267	10.5	12.8	32
33.5	235	309	10.0	12.5	30
45	255	314	10.0	12.5	25

Table 2: Mechanical properties of cold-worked Al-6063 as a function of the thermal neutron fluence

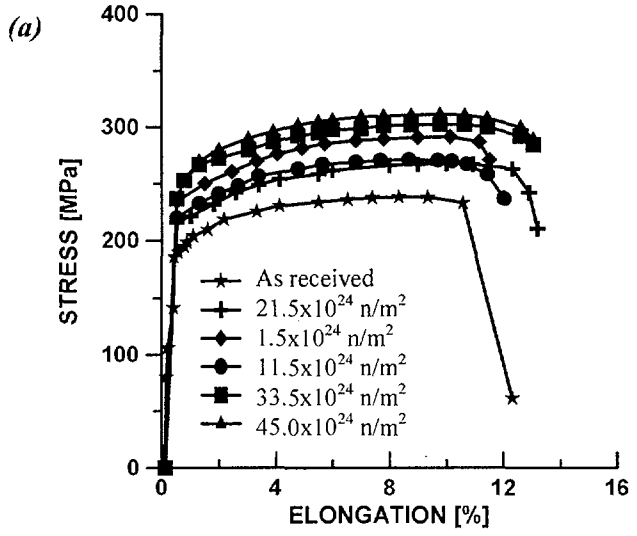

Fig. 2. Stress-strain curves of Al-6063 samples as function of thermal neutron fluences (a) and annealing time (b).

Table 3: Mechanical properties of cold-worked Al-6063 as a function of aging duration at 52°.

Aging duration [months]	Stress		Elongation		Final area reduction [%]
	σ_Y [MPa]	σ_{UTS} [MPa]	Uniform [%]	Total [%]	
0	189	238	7.9	11.9	73
1	189	240	9.8	13.2	72
2	202	258	10.6	13.2	73
6	222	282	11.1	12.8	50
8	229	289	11.1	12.9	51
13	234	293	11.1	12.85	45
15	228	287	11.9	14.2	42
18	245	304	11.8	12.5	37
22	242	300	10.8	12.5	37
24	243	301	11.0	12.2	35
27	247	306	11.1	12.7	30
30	245	302	10.9	11.3	27

The mechanical properties of unirradiated samples which were subjected to a 2.5-year annealing at 52° showed similar changes in mechanical properties as occurred during irradiation, (see Table 3 and Figure 2b).

4.2 Fractography

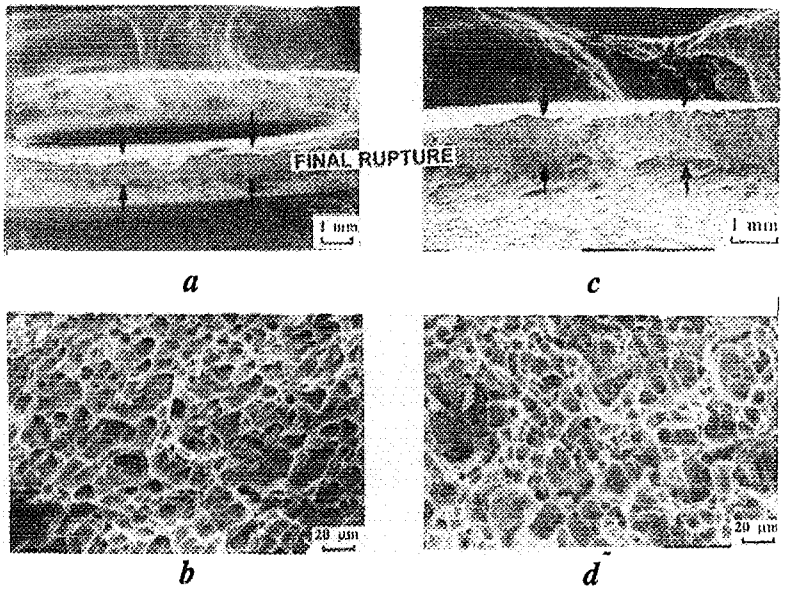

Fig. 3: Secondary electron images illustrating the fracture morphology of 23% cold-worked Al-1050 specimens before irradiation (a-b), and after irradiation to $8x10^{25}$ thermal neutrons/m^2 (c-d).

The impact of irradiation on the fracture morphology of the fractured Al-1050 specimens irradiated up to $8x10^{25}$ thermal neutrons/m^2 is illustrated in Figure 3. The fracture surfaces for unirradiated as well as for irradiated Al-1050 exhibited a transgranular dimpled shear rupture microstructure (ductile fracture) independent of the fluence (ct. Figure 3b and Figure 3d). The final area reduction of the fracture was not affected by irradiation, and its values remained above 90%.

The impact of irradiation on the fracture morphology of Al-6063 specimens irradiated up to $4.5x10^{25}$ thermal neutrons/m^2 is illustrated in Figure 4. Two major changes occurred: reduction of the final area fracture, and fracture

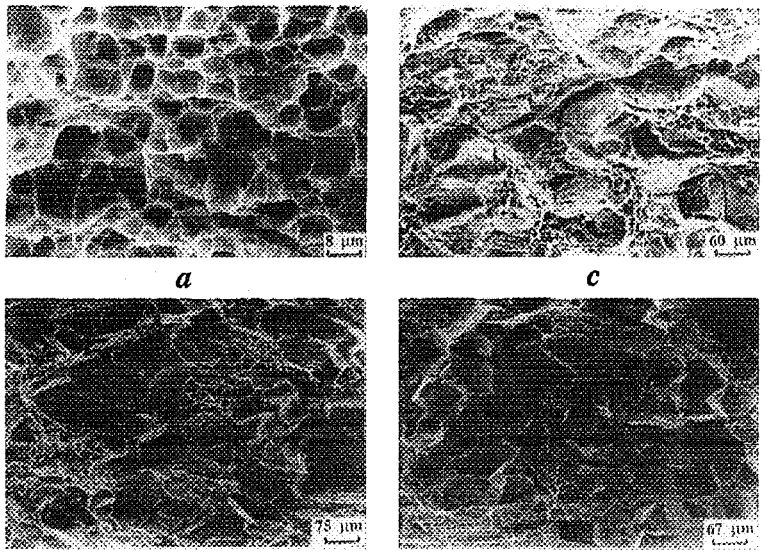

Fig. 4: Secondary electron images illustrating the fracture morphology of 23% cold-worked Al 6063 irradiated to different thermal neutron fluences. (a) unirradiated sample. (b) irradiated to $1x10^{25}$ thermal neutrons/m^2. (c) irradiated to $2.5x10^{25}$ thermal neutrons/m^2 (d) irradiated to $4.5x10^{25}$ thermal neutrons/m^2.

morphology. There was an increase in the final fracture thickness (i.e., decrease of the area reduction of the final rupture) with increasing thermal neutron fluence. For example, the final area reduction for unirradiated samples was approximately 80%. Irradiation to fluences of $1.0x10^{25}$

and $2.7x10^{25}$ thermal neutrons/m^2 led the local area reduction to 42% and 32%, respectively. A picture at a higher magnification (Figure 4) presents an even better view of the irradiation impact on the fracture morphology. The fracture of the unirradiated samples exhibits a transgranular dimpled shear rupture microstructure (Figure 4a), characteristic of a ductile fracture. After irradiation, the fracture morphology changed to a mixture of transgranular dimpled shear rupture and intergranular dimpled rupture, the latter appearing as large facets. The fraction of the intergranular rupture areas increased with the thermal neutron fluence. Similar behavior of fracture morphology was observed for prolonged annealing at 52°, as illustrated in Figure 5. Larger magnification of the facets observed in both cases reveals the dimpled structure seen in Figure 6. The dimple size is one order of magnitude smaller than the one revealed in the shear transgranular rupture.

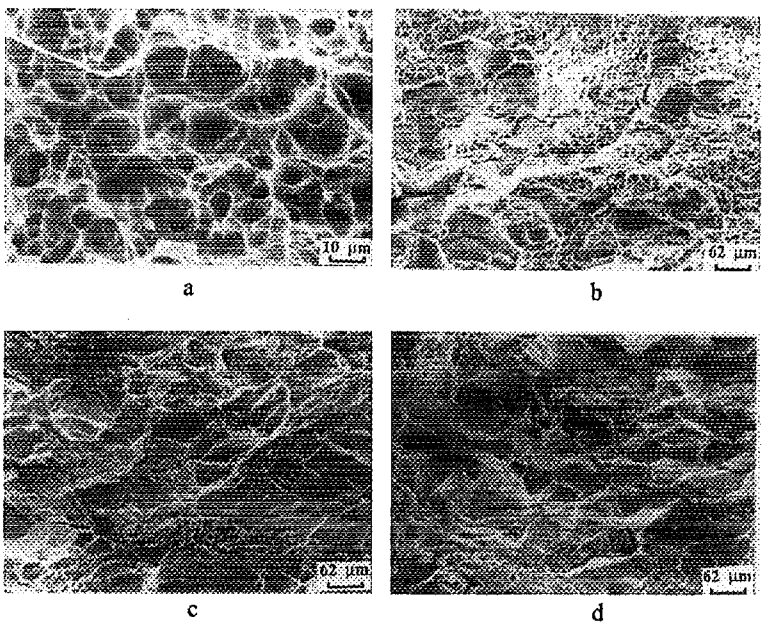

Fig. 5: Secondary electron images illustrating the fracture morphology of 23% cold-worked Al 6063 annealed for different durations. (a) before annealing (b) annealed for 6 months. (c) annealed for 15 months. (d) annealed for 30 months.

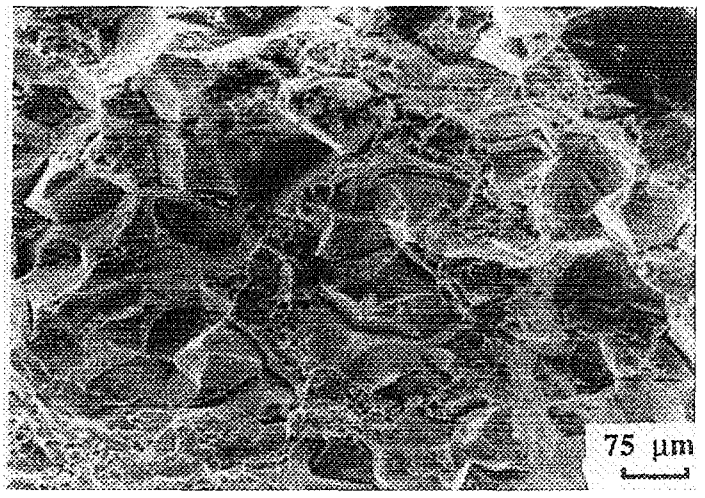

a

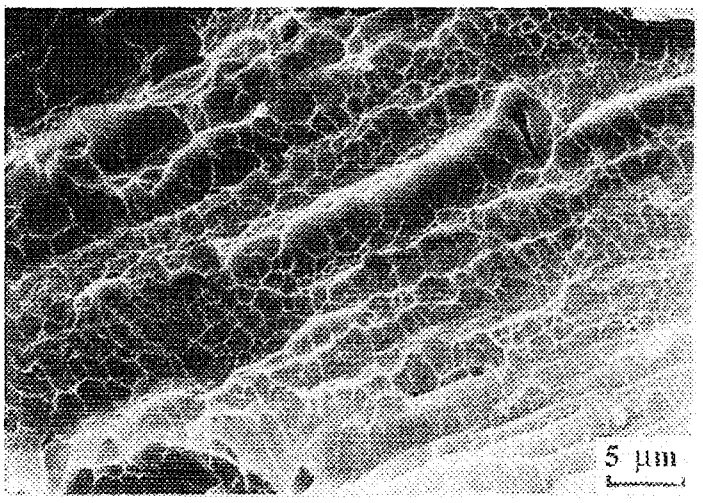

b

Fig. 6: Secondary electron images illustrating the faceted nature of fracture at two magnifications for cold-worked Al 6063 irradiated to $2.5x10^{25}$ thermal neutrons/m^2.

4.3 Irradiation impact on the internal microstructure

4.3.1 Internal microstructure of Al-1050

Irradiation of cold-worked Al-1050 causes two main microstructural changes, which are revealed under proper Bragg diffraction conditions:

(i) A decrease in dislocation density with thermal neutron fluence, as illustrated in Figure 7. The microstructure of the unirradiated specimens exhibits tangled dislocations and no individual dislocation can be distinguished (Figures 7a and 7b). After irradiation, the dislocation density decreases with thethermal neutron fluence and individual dislocations can be observed (Figures 7e and 7f). In addition, irradiation induces dislocation

rearrangement in sub-grains. The average sub-grain boundary decreases due to irradiation from 1.5 μm for the unirradiated Al-1050, to 0.5 μm for the irradiated materials under the maximum thermal fluence.

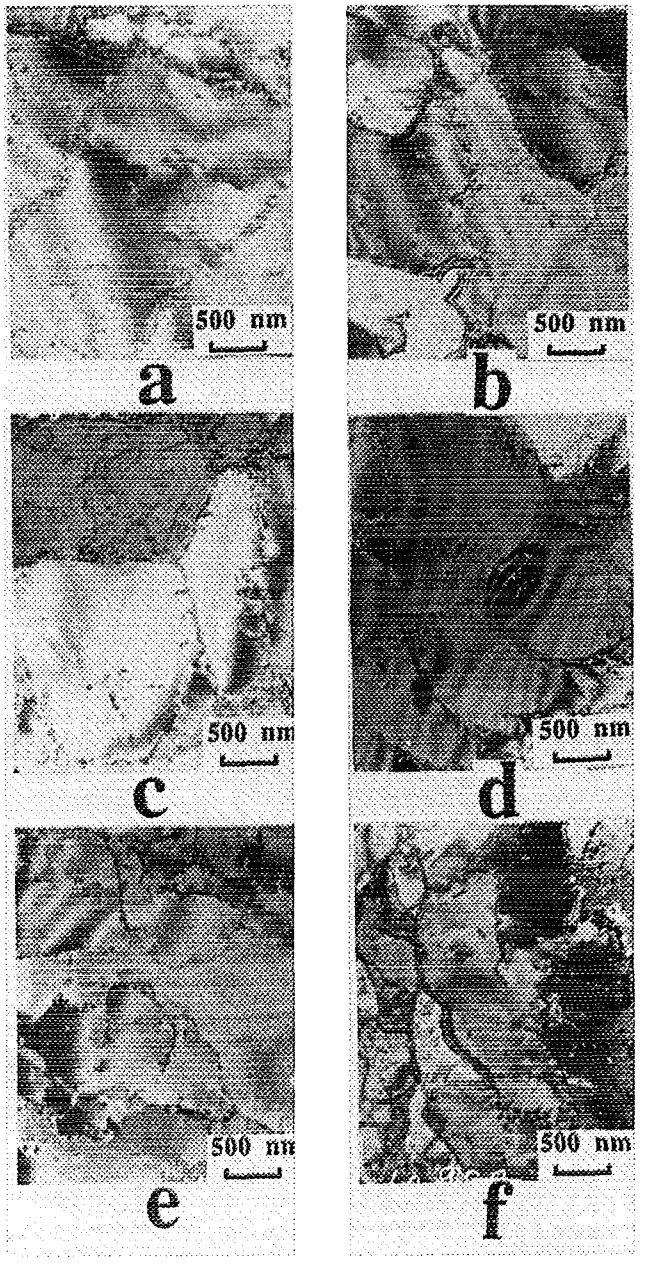

Fig. 7: Transmission electron images of 23% cold-worked Al-1050 illustrating the dislocation structure as a function of irradiation. (a-b) unirradiated samples. (c-d) irradiated to $1.4x10^{25}$ thermal neutrons/m^2. (e-f) irradiated to $2.7x10^{25}$ thermal neutrons/m^2.

ii) Irradiation-induced Si precipitation, as illustrated in Figure 8. Due to the (n,γ) interaction followed by a β decay, an Al atom transforms into Si. Silicon, however, is immiscible in the Al lattice at the irradiation temperature, and therefore precipitates as pure Si. The

average precipitate size, average distance between precipitates and precipitate density for the different fluences are summarized in Table 4. Up to the maximum thermal neutron fluence exercised, voids formation was not observed.

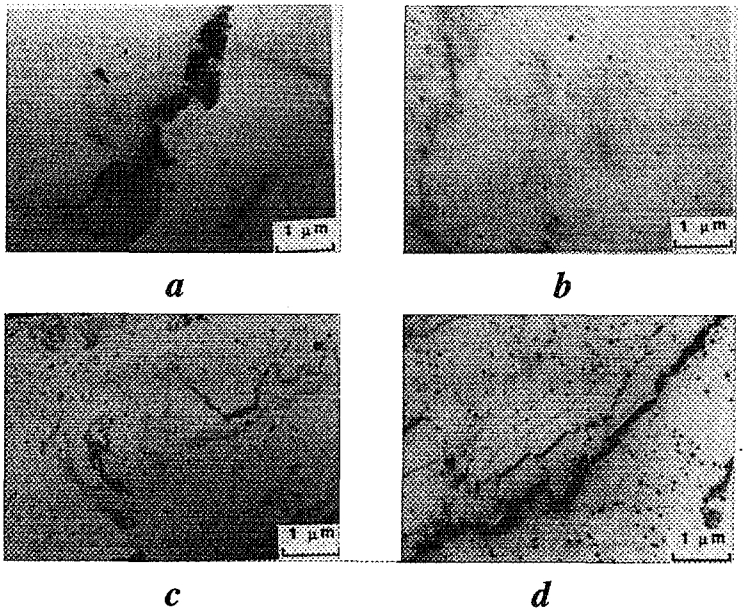

Fig. 8: Transmission electron images of 23% cold-worked Al-1050 irradiated to different fluences demonstrating the Si particle distribution. (a to d) $1x10^{25}$, $2x10^{25}$, $5x10^{25}$ and $8x10^{25}$ thermal neutrons/m^2, respectively.

Fluence [10^{25}/m^{25}]	Density, C [particles/m^3]	Particle size, d [nm]	Inter-particle distance, x [nm]
1			
2	$1.25x10^{19}$	34	230
3	$7.90x10^{19}$	34	90
5	$8.90x10^{19}$	37	80
8	$25.40x10^{19}$	41	76

Table 4: Average particle size, average distance between Si particles and particle density in cold-worked Al-1050 for different thermal neutron fluences.

4.3.2 Internal microstructure of Al-6063

Similarly to the case of Al-1050, irradiation of cold-worked Al-6063 induces microstructural changes, as illustrated in the TEM in Figure 9. A decrease occurred in dislocation density with thermal neutron fluence. The microstructure of the unirradiated specimens (Figure 9a) shows tangled dislocations, and no individual dislocation can be distinguished. After irradiation, the dislocation

density decreased (Figures 9c to 9d), and individual dislocations could be resolved. In addition, as suggested by the observed increase in material strength, precipitation of Mg_2Si probably increases with irradiation fluence. However, no individual precipitates were observed.

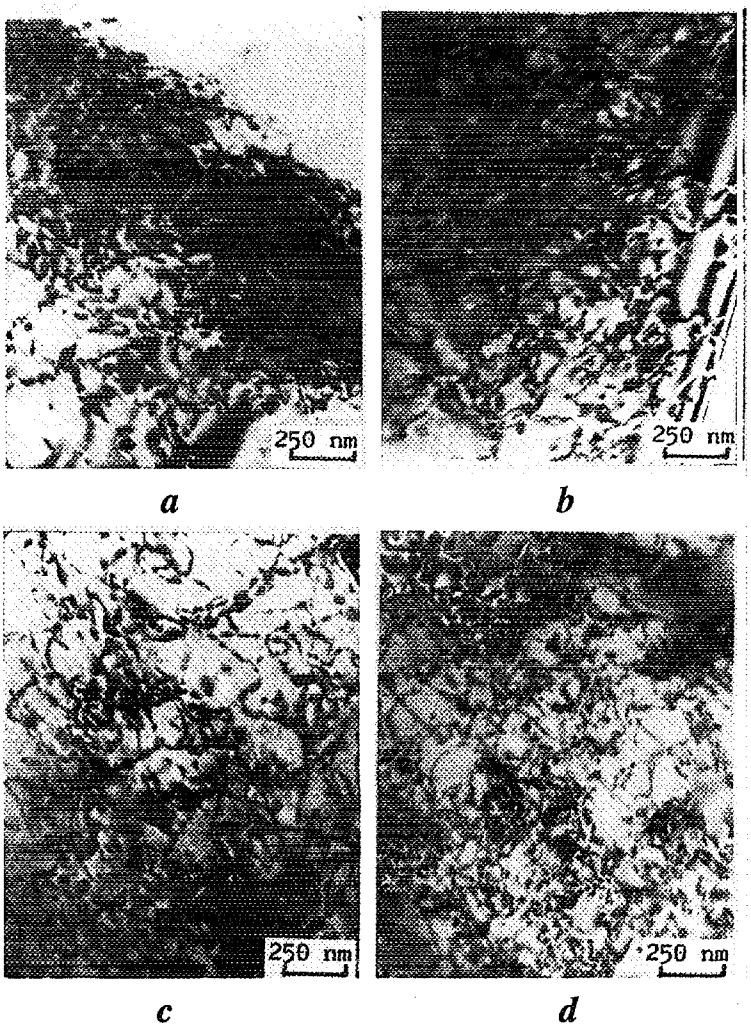

Fig. 9: Transmission electron images of 23% cold-worked Al6063. (a) annealed to 500°C for 4 hrs. (b) 23% cold-worked unirradiated samples. (c) irradiated to $2.0x10^{25}$ thermal neutrons/m^2. d) irradiated to $4.5x10^{25}$ thermal neutrons/m^2.

Irradiation also induces the formation of Precipitation Free Zones (PFZ) along both sides of the grain boundaries, as demonstrated in Figure 10. No voids were observed up to the maximum thermal neutron fluence exercised.

Fig. 10: Transmission electron image illustrating the onset of PFZ formation at grain boundaries 23% cold-worked Al6063 irradiated to $4.5x10^{25}$ thermal neutrons

5. Discussion

Al-1050, which is considered a commercially pure aluminum, in fact contains 0.5 wt.% of additional elements (Fe and Si are the major impurities) whereas Al-6063, which is considered as an alloy contains approximately 0.4, 0.5 and 0.2 wt.% of Fe, Mg and Si, respectively. Therefore, Al-6063 undergoes aging whereas Al-1050 does not. This difference in behavior influences the mechanical propertiesand the internal microstructure of the two alloys. For example, the fracture morphology of irradiated Al-1050 remains transgranular dimpled, whereas in a contrast, irradiation of Al-6063 causes a change from a transgranular dimpled structure to a mixed transgranular-dimpled and intergranular-dimpled structure.

5.1 The impact of neutron irradiation on mechanical properties

Under our irradiation conditions, neutron irradiation of cold-worked Al-6063 resulted in an increase in yield stress, as well as an increase in ultimate tensile strength and elongation. The same behavior was observed after irradiation of cold-worked Al-1050 [17]. Generally, neutron irradiation induces changes in precipitation, dislocation density, and void formation, all of which contribute to the strengthening of the irradiated material. In our studies, no voids could be observed up to the maximum thermal neutron fluence to which both Al types were exposed. Rather, irradiation caused a decrease in the dislocation density, indicating partial Al recovery, which increases elongation and decreases the ultimate tensile strength.

The impact of annealing on the ultimate tensile strength (σ_{UTS}) after irradiation is more pronounced in Al-1050. First, the σ_{UTS} drops below the unirradiated value (123 MPa) to 95 MPa for a fluence of $1x10^{25}$ thermal neutron/m^2; then it rises with irradiation to 133 or 142 MPa for fluences of $5x10^{25}$ or $8x10^{25}$ thermal neutron/m^2, respectively. However, as we shall see later, this increase can be ascribed to irradiation-induced Si precipitation, as seen in Figure 8. In contrast to Al-1050, irradiation-induced precipitation does take place in the case of Al-6063. It is well known that in Al-Si-Mg alloys like Al-6063 Mg_2Si precipitation can be detected only at full aging (T6)[20] and therefore, it is not surprising that no precipitates could be observed in the case of this alloy. However, their influence on the mechanical properties was observed, as evidenced by an increase in the yield stress and in the ultimate tensile strength. The presence of precipitates is also evidenced by the onset of formation of precipitation free zones (PFZ) near

the grain boundary, as demonstrated in Figure 10.

The overall change in the tensile strength and elongation of the irradiated alloy reflects the superposition of all the afore mentioned effects. It seems that, in the case of elongation, the contribution of the recovery is dominant, whereas precipitation hardening exerts the dominant effect on the increase in ultimate tensile strength. Thus, irradiation induces an increase in ultimate tensile strength, which is accompanied by a decrease in elongation[21]. Our results agree well with studies indicating that annealing of cold-worked Al-1100 [15] and Al-6061[1] may take place during irradiation.

Theoretically, each strengthening mechanism contributing to the change in ultimate tensile strength may be calculated as a function of the precipitation density, average precipitation size, dislocation density, and void size and density[14]. However, in the case of Al-6063 these parameters are difficult to estimate and therefore only the general trend can be discerned. Quantitative evaluation requires development of a model and a special method that should allow an exact weighing of dislocation and precipitation. We are presently engaged in the development of such a method. In contrast, in Al-1050 only Si particles precipitate and these particles are much larger than those of Mg_2Si, therefore their contribution to hardening may be calculated as follows:

The change in the yield stress due to irradiation $\Delta\sigma_y$ may be expressed as:

$$\Delta\sigma_y = \Delta\sigma_{Si} + \Delta\sigma_v + \Delta\sigma_d \qquad (1)$$

where $\Delta\sigma_{Si}$, $\Delta\sigma_v$ and $\Delta\sigma_d$ are the separate contributions to $\Delta\sigma_y$ by Si precipitates, voids and dislocations, respectively.

For Al-1050, the increase in yield stress is approximately equal to the corresponding increase in the ultimate tensile strength[22], i.e., $\Delta\sigma_{UTS} \cong \Delta\sigma_y$. Therefore, in the case of this Al alloy eq. (1) accounts also for the dependence of the ultimate tensile strength on $\Delta\sigma_{Si}$, $\Delta\sigma_v$ and $\Delta\sigma_d$ (It is worth mentioning in this context that our instrumentation provided a reliable reading of the ultimate tensile strength but not of the yield stress).

Void formation was not detected under our experimental conditions, indicating that $\Delta\sigma_v=0$. As mentioned previously, Si starts to precipitate only after an incubation irradiation of approximately $1x10^{25}$ thermal neutrons/m^2, whereas a decrease in dislocation density which causes a decrease in the ultimate tensile strength was observed at all fluences. As soon as Si starts precipitating, it provides a positive contribution to the ultimate tensile strength (eq.(1)). At $2x10^{25}$ thermal neutrons/m^2 this contribution is sufficiently large to compensate for the negative contribution of $\Delta\sigma_d$ (see Table 5).

Thermal neutron fluence [a]	Experimental σ_{UTS} [MPa]	$\Delta\sigma_{Si}$ [MPa]	Calculated σ_{UTS} [MPa]
1	95		95
2	---	5±3	---
3	106	14±7	109+7
5	133	16±8	111+8
8	142	28±15	123+15

Table 5: Experimental and calculated (σ_{UTS} =95+$\Delta\sigma_{Si}$ [MPa] ultimate tensile strength of irradiated Al-1050 for different thermal neutron fluences.

The increase in the ultimate tensile strength of Al1050, caused by the interaction of mobile dislocations with silicon precipitates derived from the dispersed-phase hardening theory [11], is expressed by equation 2:

$$\Delta\sigma_{Si} = 1.04/\pi(Gb)(Cd)^{1/2}\ln(d/(4b)) \qquad (2)$$

where G is the shear modulus of aluminum (2.648×10^4 MPa), b is the Burger,s vector (0.286 nm), and C is the precipitate density of average diameter d. Substitution of the experimental values of C and d from Table 2 enables evaluation of the increase in the ultimate tensile strength for Si precipitation and yields the results presented in Table 5, in which the specified error limits reflect uncertainties in sample thickness and the measured precipitate density. The maximum increase in the $\Delta\sigma_{UTS}$ values calculated using expressions 1 and 2 ranges between 28 and 43 MPa.(Table 5) which, within the experimental error, is quite close to the increase in experimentally measured σ_{UTS} values.

5.2 The impact of prolonged aging on mechanical properties.

It appears that neutron irradiation and low-temperature-prolonged aging play an important role in determining the post-irradiation mechanical properties of the aluminum alloys. In the case of Al-6063, prolonged aging has a similar effect on the mechanical properties as does irradiation (compare Figure 2 and Table 2 with Figure 3 and Table 3). Therefore, it is reasonable to assume that under our irradiation conditions, annealing and aging are the dominant factors influencing the microstructural and mechanical properties, due to the temperature field generated during irradiation. However, it should be noted that during irradiation, Si is also formed from Al by the Al(n,γ)Si nuclear reaction. The presence of Si might increase the

strengthening during irradiation by increasing precipitation of Mg_2Si or of pure Si.

Since aging and annealing of the Al parts inside the reactor depend on the irradiation duration, the neutron flux may be a very important factor in determining the mechanical properties of these parts. A large thermal neutron flux (of the order of 10^{18}-10^{19} thermal neutrons/(m^2s) entails a large Si creation rate, as well as a shorter exposures to the aging temperature. There appears to be the need for an incubation period of 2 to 3 months before the changes in the mechanical properties induced by annealing can be observed (see Table 2). Thus, for low fluxes (of the order of 10^{16}-10^{17} thermal neutrons/(m^2s), as in our case, thermal aging during irradiation would seem to be the major factor influencing the mechanical properties of aluminum. In contrast, in a High Flux Isotope Reactor (HFIR), where the irradiation duration required to obtain fluences of the order of 10^{25}-10^{26} thermal neutrons/m^2 is of the order of several months, irradiation effects like atom displacements, dislocation, and voids formation become predominant.

The impact of Al-1050 low temperature annealing during irradiation is also dominant in determining its post-irradiation mechanical properties. However, Si precipitation, which takes place in this case, is larger and less dense than that observed for Mg_2Si. and as pointed out in the next section, PFZ would not form under these conditions. Therefore, fracture morphology of Al-1050 is expected to remain unchanged during irradiation.

5.3 The Impact of Precipitation Free Zone on Fracture Morphology

At first sight, the changes that take place during irradiation appear to have an opposing effects on the mechanical properties of the alloy: (i) an increase of uniform elongation with thermal neutron fluence, which indicates an increase in ductility; and (ii) a decrease in elongation, as indicated by the diminished of local area reduction accompanied by an increase in the density of intergranular facets.

It is well known that Al-Mg-Si alloys, like Al-6063, undergo a sequence of precipitation stages: Guinier-Preston (G. P.) Zones-→θ"-→θ'-→θ. The G.P. Zones are actually locally Mg-enriched regions, which then transform to a coherent θ" precipitation consisting of metastable Mg_2Al precipitates. However, it is difficult to detect these precipitates in Al-Mg-Si[20] before a fully aged condition (T6) is reached after which time the precipitates become semi-coherent (θ' precipitate) and visible. In this process, (PFZ) around the grain boundary is usually created. There are two main reasons for creating a PFZ adjacent to a grain boundary: (i) Mg diffusion into the grain boundary and the formation of Mg_2Si precipitation at the grain boundary; and (ii) enhanced vacancy diffusion to the grain boundary, resulting in the creation of a denuded vacancy. It is well known that in a region of small vacancy concentration, it is difficult to cause precipitation.

We have found evidence that PFZs begin to form during irradiation, as seen in Figure 8. These PFZ regions are responsible for the creation of the dimpled intergranular fracture, as well as the increase in the homogeneous elongation. Due to precipitation, the grains become stronger

and therefore a higher stress is required for necking. Increase in the ultimate tensile stress, as has been found by the examination of mechanical properties, is expected to cause an increase in the uniform elongation. On the other hand, the PFZs are weaker than the grains; hence, at a certain stress, they will rupture throughout the PFZ, but not necessarily at the grain boundary. As may be seen in a well developed PFZ, obtained in an Al-6063 alloy under T6 aging conditions, needle precipitation protrudes into the PFZ, and is the source of the dimpled nature of the fracture. Actually, under fully aged conditions, the entire cross-section structure is intergranular dimpled[22]. Thus, it is hard to say that the presence of a transgranular dimpled structure is typical of a brittle fracture. In addition, the local area reduction decreases, due to ductility losses in the grains at the necking regions.

Conceivably, Alexander's[23] observation of large crack propagation in spite of only minor changes in the fracture toughness, may be attributed to the formation of PFZs. A similar explanation of the fracture morphology was given by Sturcken[13].

6. Conclusions

The effects of irradiation of cold-worked Al-1050 and Al-6063 in a thermal reactor are as follows:

a. Radiation-induced recovery of cold-worked samples, as evidenced by a decrease in dislocation density and an increase in elongation.

b. No voids are observed up to a fluence of 8×10^{25} thermal neutrons/m^2 ($E < 0.625$ eV).

c. A decrease in local area reduction at rupture occurrs with Al-6063 whereas for Al-1050 it remains unchanged.

The major factor influencing the microstructure and mechanical properties during irradiation is prolonged thermal annealing caused by the temperature field generated during irradiation.

Annealing of cold-worked aluminum alloys at 52° for long periods of time has the same effects as neutron irradiation. In both cases, the fracture morphology changes from a transgranular shear rupture to a mixture of transgranular dimpled shear rupture and intergranular dimpled rupture. The fraction of the intergranular rupture area increases as a function of the thermal neutron fluence.

Unlike Al-6063, the fracture morphology for Al-1050 remains unchanged when subjected to thermal annealing.

7. References

1. R. T. King and A. Jostsons, Metall. Trans. A, **6a**, 863 (1975).
2. H. E. McCoy, Jr., and J. R. Weir, Jr, Nucl. Sci. Eng. **25**, 319, (1966).
3. R. T. King, E. L. Long, Jr., J. O. Stiegler and K. Farrell, J. Nucl. Mater. **35**, 231, (1970).
4. K. Farrell, A. Wolfenden and R. T. King, Radiat. Eff. **8**, 107, (1971).
5. N. H. Packan, J. Nucl. Mater. **40**, 1 (1971).
6. A. Jostsons, and E, L. Long, Jr., Radiation Effects **16**, 83 (1972).
7. K. Farrell and R. T. King, Metall.. Trans. **4**, 1223, (1973).
8. R. T. King, A. Jostsons and K. Farrell. Effects of radiation on structure and mechanical properties of metals and alloys., Proc ASTM STP 529, American Society for Testing and Materials, 1973, pp. 165-180.
9. K. Farrell, and A. E. Richt,. Properties of reactor structural alloys after neutron particle irradiation, ASTM STP 570, Proc. American Society for Testing and Materials, Symposium on the effects of radiation on structural material, Gatlinburg, Tennessee, USA, 11 Jun 1974, Published 1975, pp. 311-325.
10. K. Farrell, and A. E. Richt, "Microstructure and tensile properties of heavily irradiated 1100-0 aluminum". 9 th symposium on effects of radiation in stuctural materials, Washington, USA, 10-14 July 1978, p. 19.

11. K. Farrell and A. E. Richt, in "Effects of radiation on structural materials", J. A. Sprague and D. Kramer Eds., Proc. ASTM STP 529, Americal Society for Testing and Materials, Los Angeles, California, 26 Jun 1972, Published 1973, pp. 427-439.

12. K. Farrell, and T. King, "Symposium on Effects of Radiation in Structural Materials", (Richland, WA, USA, 11-13 July 1978) ASTM STP 683, J. A. Sprague and D. Kramer, Eds. American Society for Testing and Materials, 1979, pp. 440-449.

13. E. F. Sturcken, J. Nucl. Mater., **82**, 39 (1979).

14. K. Farrell, J. Nucl. Mater. **97**, 33 (1981).

15. H. Yoshida, Kozuka, and T. Sagane, "The 24th Japan Congress on Materials, Research-Metallic Materials", Research Reactor Institute, Kyoto University, Japan, 1981, pp. 1-6.

16. E. Lijbrink, H. J. Van Grol, F. Dekker, W. van Witzenburg, in: 11th Inter. Symp on "Effects of radiation on materials":. (volume II), ASTM STP 782, H. H. Brager and S. Perrin, Eds. American Society for Testing and Materials, Philadelphia, 1982, pp. 765-778.

17. A. Munitz, J. Nucl. Mater.**165**, 305, (1989).

18. J. R. Weeks, C. J. Czajkowski, and P. R. Tichler, in 14th Inter. Sym "Effects of radiation on materials":. (volume II), ASTM STP 1046, N. H Packan, R. E. Stoller and A. S. Kumar, Eds. American Society for Testing and Materials, PA, USA 1982, Vol.II, pp. 441-452.

19. N. R. McDonald and C. J. Moss, "IAEA Seminar for Asia and the Pacific on Aging, Decommissioning and/or Major Refurbishment of Research Reactors", Bangkok, Thailand 18-22 May 1992.

20. L. F. Mondolfo, Aluminum Alloys: "Structure and Properties", 1976, Butterworths, London, UK, pp. 566-575.

21. A. Munitz, H. Sthechman, C. Cotler, M. Talianker, O. Beery, F. Simca, A. Sella and Z. Barkai, in: "Proceedings 7th Israel Materials Engineering Conference", Haifa, Israel, November 27-29, A. Rosen and R Chaim, Eds., pp. 529 - 535.

22. "Aluminum Standards and Data", 2nd ed., The Aluminum Association, New York, NY. 1969 p. 27.

23. D. J. Alexander, in: 16th Annual Symp. American Society of Testing and Materials (ASTM), 21-25 June 1992, CONF. 920673-19.